COMMUNICATION

Ligand-Free Ultrasmall Recyclable Iridium(0) Nanoparticles for Regioselective Aromatic Hydrogenation of Phosphine Oxide Scaffolds: An Easy Access to New Phosphine Ligands

Gaspard Hedouin,[a] Sudripet Sharma,[a] Karanjeet Kaur,[a] Ramesh Hiralal Choudhary,[a] Jacek B. Jasinski,[b] Fabrice Gallou,*[c] Sachin Handa*[a][d]

[a] Dr. G. Hedouin, Mr. S. Sharma, Ms. K. Kaur, Mr. R. H. Choudhary, Dr. S. Handa
Department of Chemistry, University of Louisville
2320 S. Brook Street, Louisville, Kentucky 40292, United States
E-mail: sachin.handa@louisville.edu
[b] Dr. J. B. Jasinski
Conn Center for Renewable Energy Research, University of Louisville
Louisville, Kentucky 40292, United States
[c] Dr. F. Gallou
Chemical & Analytical Development, Novartis Pharma AG
Basel 4056, Switzerland
E-mail: fabrice.gallou@novartis.com
[d] Department of Chemistry, University of Missouri
601 S College Ave # 125, Columbia, MO 65211, United States
E-mail: sachin.handa@missouri.edu

Supporting information for this article is given via a link at the end of the document.

Abstract: Herein, we developed the recyclable ligand-free iridium (Ir)-hydride based Ir(0) nanoparticles (NPs) for the first regioselective partial hydrogenation of P(V)-substituted naphthalenes. Both the isolated and in-situ generated NPs are catalytically active. Control nuclear magnetic resonance (NMR) study revealed the presence of metal's surface-bound hydrides, most likely formed from Ir(0) species. A control NMR study confirmed that hexafluoroisopropanol as a solvent was accountable for substrate activation via hydrogen bonding. High-resolution transmission electron microscopy of the catalyst supports the formation of ultrasmall NPs, while X-ray photoelectron spectroscopy confirmed the dominance of Ir(0) in the NPs. The catalytic activity of NPs is broad as showcased by highly regioselective aromatic ring reduction in various phosphine oxides or phosphonates. The study also showcased a novel pathway toward preparing bis(diphenylphosphino)-5,5',6,6',7,7',8,8'-octahydro-1,1'-binaphthyl (H_8-BINAP) and its derivatives without losing enantioselectivity during catalytic events.

Introduction

Hydrogenation of arenes is a direct and elegant method for preparing saturated cyclic compounds. The common issues making this reaction less attractive are the selectivity, recyclability of the reaction medium and the catalyst, and scalability. Nonetheless, selective arene hydrogenation remains a significant challenge in synthetic chemistry.[1] Compared to stereoselective hydrogenation of ketones or imines,[2] it is a less established reaction. Using cyclic (alkyl)(amino)carbene rhodium (Rh-CAAC) catalyst, chemoselective reduction of arenes containing reducible or labile functional groups have been achieved by Zeng[3] and Glorius[4] groups (Scheme 1A). In fused-heterocyclic structures, the reduction of a heteroaromatic ring is more favored due to its lower aromaticity value.[5] However, a few reports on the regioselective reduction of a non-heteroaromatic ring in such structures using ligated ruthenium catalysts have appeared in the literature (Scheme 1B).[6] Regioselective reduction of a single ring of naphthalene is more challenging and is generally dictated by the substitution—such examples remain scarce. Selective reduction of naphthols has been described by the groups of Luo and Zeng[7] and Huang.[8] In these examples, the reduction of a substituted ring was achieved. Hydrogenation of 1,1′-bi-2-naphthol (BINOL) with platinum[9] or palladium catalysts[10] using harsh conditions is also precedented. Very recently, regioselective transfer hydrogenation of a few functionalized arenes has also been reported.[11] Apart from work mentioned above, the literature lacks a methodology for the highly regioselective reduction of (naphthyl)phosphine oxide scaffolds, and also selective chemoreductions by ligand-free catalysts. Notably, often the cost of the ligand is significantly more than the metal. Furthermore, it is much easier to recycle the metal than the ligands. Aiming for the late-stage diversification of highly important bis(diphenylphosphino)-5,5',6,6',7,7',8,8'-octahydro-1,1'-binaphthyl (H_8-BINAP) ligands, we envisioned a hydrogen-bonding assisted novel pathway for regioselective reduction of

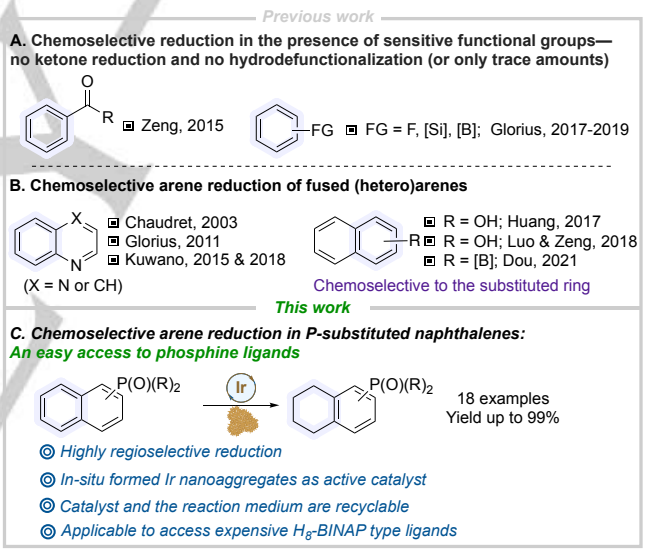

Scheme 1. (A) Chemoselective reduction of arenes; (B) Chemoselective reduction of bicyclic (hetero)arenes; (C) Regioselective reduction of P(V)-substituted (naphthyl)phosphine oxides.

(naphthyl)phosphine oxides. Herein, we described the first ligand-free regioselective hydrogenation of P(V)-substituted naphthalenes catalyzed by *in-situ* formed ultrasmall iridium (Ir) nanoparticles (NPs). This reaction tolerates diverse P(V) substituents, including phosphines and phosphonate esters. Besides, this methodology allows the rapid and facile synthesis of H_8-BINAP ligands from inexpensive 2,2′-bis(diphenylphosphino)-1,1′-binaphthalene (BINAP) precursors that could benefit researchers in academia and industry to quickly access new chiral ligands (Scheme 1C).

For the catalyst design, our findings were based on the hypothesis that when a metal salt is subjected to a hydrogen atmosphere in a lipophilic polar-protic solvent, it tends to form nanostructured catalytic material (driven thermodynamically) containing metal-hydridic species stabilized by intermolecular hydrogen bonding with solvent molecules (Figure 1). The reductive elimination of hydrogen from metal hydride generates a metal atom in a lower oxidation state that further acts as a nucleus for the formation of ultrasmall NP in the nanostructured material. In the NP, the presence of hydride on the metal surface and the site (metal in the lower oxidation state) for the selective metal-arene interaction could lead to selective reduction of the aromatic ring. The less hindered and unsubstituted flat aromatic ring in the naphthalene moiety is most likely more accessible for the metal-arene interaction.

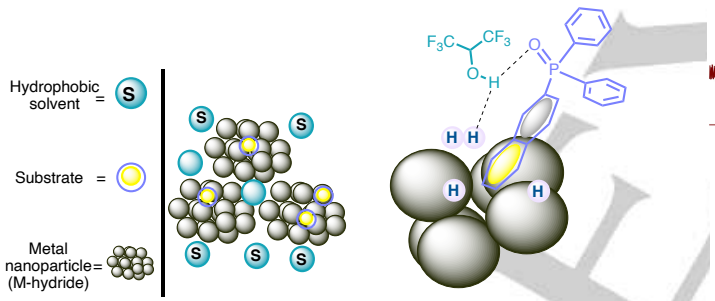

Figure 1. Metal hydride nanoparticles under hydrophobic environment.

Results and Discussion

Due to the ease of formation and more stability of Ir-hydride (Ir-H) compared to palladium-hydride (Pd-H), we selected Ir as the metal of choice for the synthesis of NPs. In addition, the large atomic radius of Ir compared to Pd could assist in the formation of hydrophobic nanostructures to promote metal-substrate interaction.[12] The large metal's surface area could also greatly assist intermolecular hydrogen bonding between substrate, solvent, and Ir-H. Based on these assumptions, we synthesized NPs containing Ir-H. The synthetic method for their formation was straightforward. Suspending the $[Ir(COD)Cl]_2$ in hexafluoroisopropanol (HFIP) and naphthalen-1-yldiphenylphosphine oxide (**1a**) and exposing the resulting mixture to a hydrogen atmosphere led to the formation of black-colored nanostructured Ir-H or NPs. After isolation, we thoroughly characterized the NPs or reaction mixture containing NPs by Infrared (IR) spectroscopy, mass spectrometry, and nuclear magnetic resonance (NMR) spectroscopy to support the mechanism of the formation of nanoclusters, existence of Ir-H, and intermolecular hydrogen bonding.

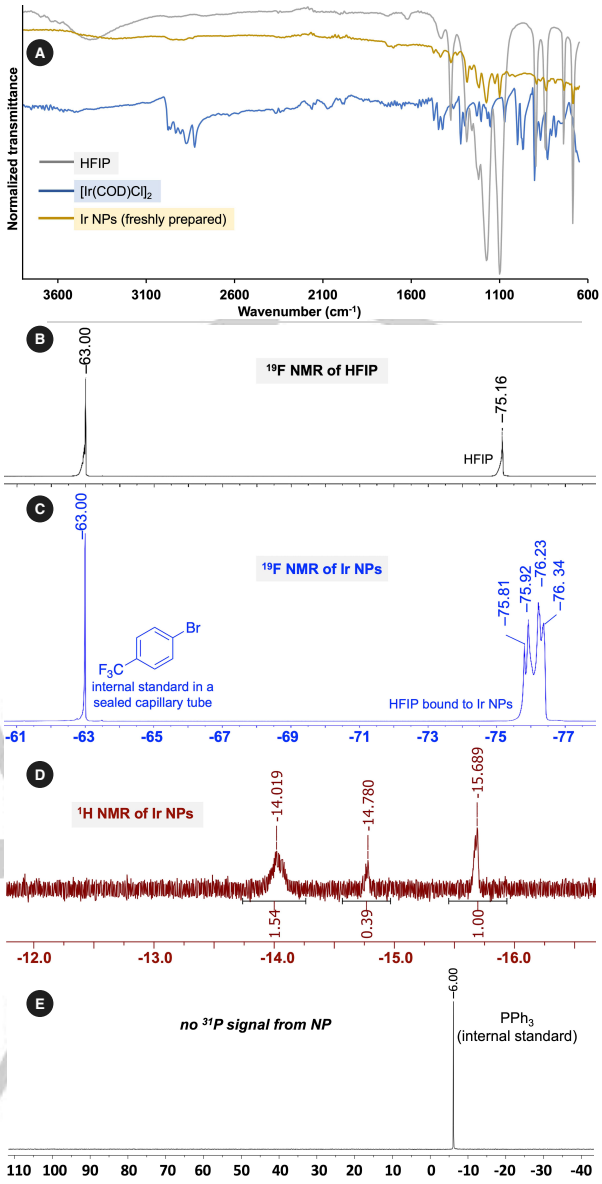

Figure 2. Iridium hydride (Ir-H) nanoparticles (NPs) under hydrophobic environment. (A) Infrared spectroscopic study of NPs; (B, C) ^{19}F nuclear magnetic resonance (NMR) study of NPs; (D) Ir-H detection by ^{1}H NMR spectroscopy; (E) ^{31}P NMR of Ir NPs for the detection of residual phosphine oxide.

The comparison of IR spectra of $[Ir(COD)Cl]_2$, HFIP, and Ir-NPs revealed an association of HFIP with the NPs (Figure 2A). As supported by IR data, cyclooctadiene (COD) is fully reduced under a hydrogen atmosphere, forming an Ir(0) atom that potentially acts as a nucleus for NP formation. ^{1}H NMR spectroscopic analysis of Ir NPs, 1,5-cyclooctadiene (COD), and $[Ir(COD)Cl]_2$ confirmed the complete reduction of COD to cyclooctane (for details, see Supporting Information, Figure S10). Neither COD nor cyclooctane was found in the NPs. Mass spectrometry of solvent after the NP formation further supported the complete reduction of COD that may be responsible for the release of Ir atom from the molecule (for details, see Supporting Information, Figure S11). ^{19}F NMR spectroscopic study also supported the binding of HFIP with NP surface (Figure 2B, C). A neat HFIP's ^{19}F signal appeared at –75.16 ppm, while signals for the NP-bound HFIP appeared at –75.81 - –76.34 ppm, indicative

of the presence of HFIP in the NP cluster. Further, the formation of hydrides of Ir was probed. ^{1}H NMR data of isolated NPs clearly supported the presence of Ir-H in the nanoclusters. Three signals at –14.02, –14.78, and –15.69 ppm were indicative of three different types of Ir-H in a 3:1:2 ratio. (Figure 2D; for details, see Supporting Information, Figure S5-S7). Notably, naphthalen-1-yldiphenylphosphine oxide (**1a**) used during the synthesis of NPs only helps to control the NP morphology. In its absence, only catalytically inactive black clumps of Ir were formed (see Supporting Information, Figure S17). However, naphthalen-1-yldiphenylphosphine oxide doesn't stay in NP, as suggested by ^{31}P NMR of NP (Figure 2E).

The scanning electron microscopy (SEM) and high-resolution transmission electron microscopy (HRTEM) analysis indicates the presence of Ir NPs with different morphologies (Figure 3A-F). Energy-dispersive X-ray spectroscopy (EDS) analysis confirmed that the Ir is the major component of NPs (Figure 3B, C). These NPs tend to make large clusters, responsible for their reduced catalytic activity (Figure S12). However, the sonication of these black colored clusters in HFIP was performed before the analysis, the resulting material was also found as catalytically active. HRTEM analysis revealed the formation of ultrasmall NPs with an average size of 1.8 nm (Figure 3D-G). X-ray photoelectron spectroscopic (XPS) analysis predominantly showed the presence of Ir(0) in the peak deconvolution spectrum of Ir4f. The majority of Ir(0) may be formed after the reductive elimination of molecular hydrogen from hydrides of Ir. A low amount of Ir(IV), likely corresponding to IrO_2, was also detected (Figure 3H, I). The oxidation of ligand-free Ir(0) happened due to air exposure of NPs. Finally, selected area electron diffraction (SAED) of the catalyst sample confirmed the crystal structure and the lattice type typical for Ir. Moreover, the lattice parameter of the catalyst sample was measured to be a_{cat} = 3.874 Å, which agrees very well (within 99% accuracy) with the 3.831 Å value reported for Ir.[13] The above analysis strongly suggest that the NPs are mainly composed of Ir(0). This oxidation state is responsible for the catalytic hydrogenation of these aromatic phosphine oxides (vide infra).

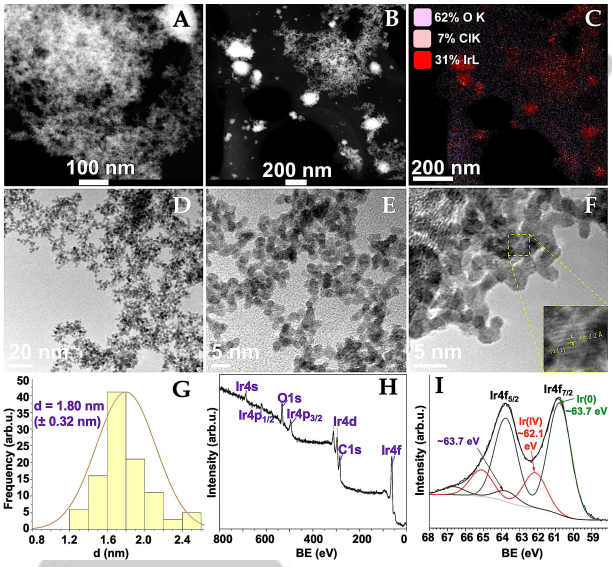

Figure 3. Analysis of Ir NPs. (A, B) scanning electron microscopic (SEM) analysis; (C) energy-dispersive X-ray spectroscopic (EDS) analysis; (D-F) high-resolution transmission electron microscopic (HRTEM) analysis; (G) average NP size; (H, I) X-ray photoelectron spectroscopic (XPS) analysis.

Table 1. Optimization of regioselective hydrogenation[a]

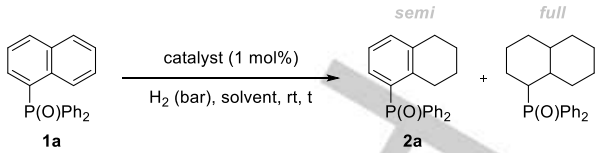

Entry	Catalyst (1 mol%)	Solvent	t (h)	Conversion (%)[b]
1[c]	$[Ir(COD)Cl]_2$	HFIP	20	66
2[c]	$[Ir(COD)Cl]_2$	1,2-DCE	20	22
3[c]	$[Ir(COD)Cl]_2$	Hexane	20	0
4[c]	$[Ir(COD)Cl]_2$	MeOH	20	28
5[c]	$[Ir(COD)Cl]_2$	HFIP (0.1 M)	20	29
6[d]	$[Ir(COD)Cl]_2$	HFIP	20	0
7[e]	$[Ir(COD)Cl]_2$	HFIP	20	43
8[f]	**$[Ir(COD)Cl]_2$**	**HFIP**	**48**	**> 99**
9	Pd/C	HFIP	20	0
10	Pd black	HFIP	20	0
11[c]	$[Rh(COD)Cl]_2$	HFIP	20	20
12[c]	$Rh(PPh_3)_3Cl$	HFIP	20	15

[a]Conditions. **1a** (0.15 mmol), H_2 (30 bar), HFIP (0.5 M), rt. [b]Conversion based on ^{1}H-NMR or ^{31}P-NMR. [c]ratio semi:full > 20:1. [d]H_2 (1 bar). [e]H_2 (10 bar). [f]ratio semi:full = 9:1.

Next, we employed our catalyst for the selective remote aromatic ring reduction of the naphthyl group in **1a**. For the sake of simplicity, we preferred using in-situ generated NPs. To our delight, our in-situ generated Ir-H NPs (derived from 1 mol% $[Ir(COD)Cl]_2$ in HFIP afforded desired product **2a** in 66% yield in 20 hours (Table 1, entry 1). The desired product **2a** could be obtained in high regioselectivity as hydrogenation of the remote ring was observed. To boost the selectivity and activity, we further fine-tuned reaction parameters, including solvent, reaction temperature, and NPs in-situ derived from other metals. Regarding desired reactivity, dichloroethane (DCE) solvent was inferior compared to HFIP, and only 22% conversion was observed (entry 2). The catalytic reaction in more lipophilic solvent hexane did not proceed (entry 3). The reaction in methanol was also slow, and only 28% conversion was achieved (entry 4). The prolonged reaction time in methanol did not improve the yield, possibly due to catalyst deactivation. Nonetheless, it indicates both hydrophobicity, hydride stability, and substrate activation via solvent-assisted hydrogen bonding are crucial for the catalytic activity. Thus, we further proceeded to optimize the conditions in HFIP solvent. Reaction concentration diluted to 0.1 M had a negative impact on the conversion of **1a**, and only 29% desired product was observed (entry 5). High pressure of hydrogen gas was necessary as either no conversion or a lower conversion was observed when 1 bar or 10 bar of hydrogen pressure was employed (entries 6, 7). Global concentration 0.5 M and H_2 pressure 30 bar were optimal, and the reaction was completed in 48 h at rt (entry 8). Isolated NPs under these conditions were also equally active. We compared the activity of our Ir-H NPs with other state-of-the-art catalysts or NPs of rhodium (Rh), but none of them

worked well. Palladium on charcoal and palladium black were inactive for the desired transformation (entries 9, 10). NPs derived from $[Rh(COD)Cl]_2$ (1 mol%) or Wilkinson's catalyst only afforded 20% and 15% conversions, respectively (entries 11, 12). Thus, Ir catalyst is superior compared to the Rh and Pd-based catalysts.

Table 2. Substrate scope for hydrogenation of P(V)-substituted naphthalene scaffolds[a]

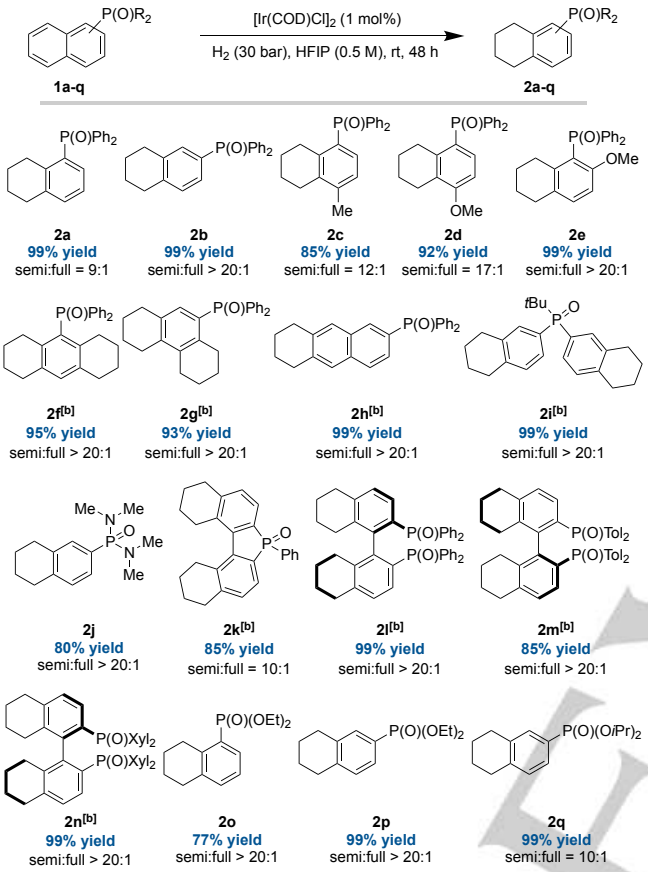

[a]Conditions. Substrate **1** (0.15 mmol), in-situ formed Ir-H NPs derived from 1 mol% $[Ir(COD)Cl]_2$, HFIP (0.5 M), H_2 (30 bar), rt, 48 h. [b]Ir-H NPs derived from 2 mol% $[Ir(COD)Cl]_2$. All reported yields are isolated yields.

Using the optimized protocol, the substrate scope of this reaction was investigated (Table 2, **2a-q**). Using naphthalen-2-yldiphenylphosphine oxide **1b**, the desired selectively reduced product **2b** could be afforded in quantitative isolated yield. Switching the diphenylphosphine oxide substituent to the second position of the naphthalene did not impact the reactivity of the catalytic process, and **2b** was also obtained in a quantitative yield. The substrates containing electron-donating groups, such as methyl and methoxy, *para* to the phosphine substituent, also worked well under the optimized protocol—the desired products **2c** and **2d** were obtained in excellent yields. Likewise, the substrate with methoxy substituent ortho to the phosphine oxide groups afforded quantitative yield (**2e**), indicating that the substituent at the proximal ring of naphthalene is not significantly impacting the selectivity and reactivity. In terms of the diversity of polyaromatic rings, more than one aromatic ring could be reduced, providing access to diverse phosphine scaffolds, as shown with the products **2f** and **2g**. Only single-ring reduction can also be achieved in an anthracene ring of **2h**—it indicates that the ring reduction is more feasible for the ring located remote to the phosphine oxide substituent. The substrate bearing hindered *tert*-butyl group could also be reduced to obtain product **2i** in quantitative yield. Notably, selective reduction at the two different naphthyl rings was achieved in this example. The regioselective hydrogenation could also deliver phosphonamide as the product **2j** was obtained in good yield. More importantly, this methodology could also provide selective hydrogenation in fused binaphthyl phosphine oxide. In the formation of **2k**, no five-membered ring opening was observed, and desired product was obtained in excellent yield. Furthermore, this catalytic process provides facile access to H_8-BINAP-type ligands, as showcased for the hydrogenation of 2,2′-bis(diphenylphosphine oxide)-1,1′-binaphthalene (BINAPO) derivatives. H_8-BINAPO **2l** and its derivatives **2m** and **2n** could be produced in quantitative yields. Most notably, no racemization was observed during the catalytic events, and the desired product retained the original enantioselectivity (for details, see Supporting Information, page S23). This novel pathway could be an alternative strategy to circumvent the lengthy preparation of H_8-BINAP ligands and their derivatives, potentially reducing the cost of these valuable ligands.[14] The selective hydrogenation of naphthyl phosphonates was also accomplished to produce **2o**, **2p**, and **2q** in high yields, demonstrating the reactions' diversity.

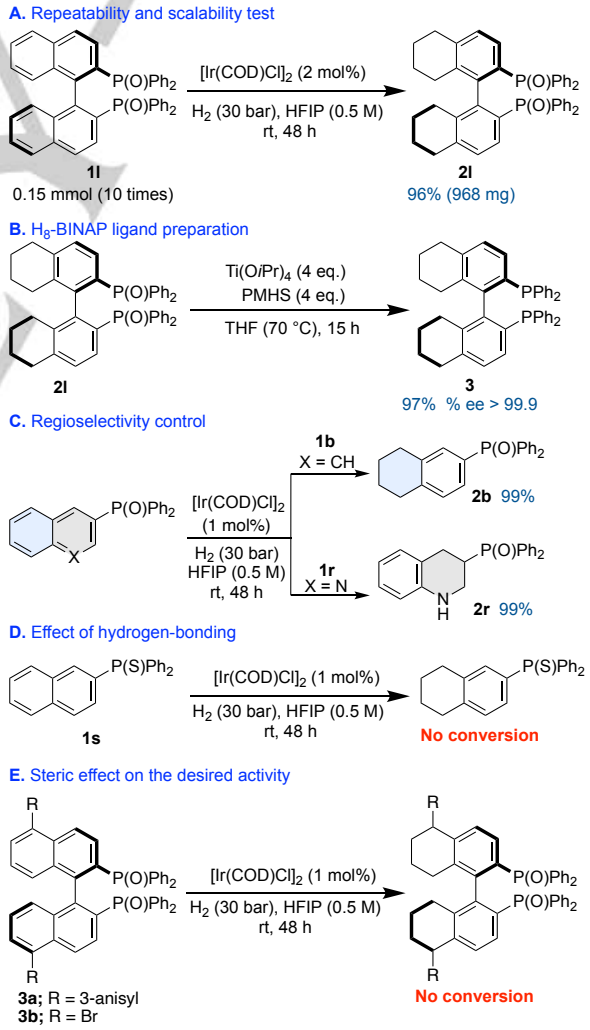

Scheme 2. (A). Repeatability experiment; (B) phosphine synthesis; (C, D) parameter control for the regioselective hydrogenation; (E) substituents on the distal ring impacting reactivity.

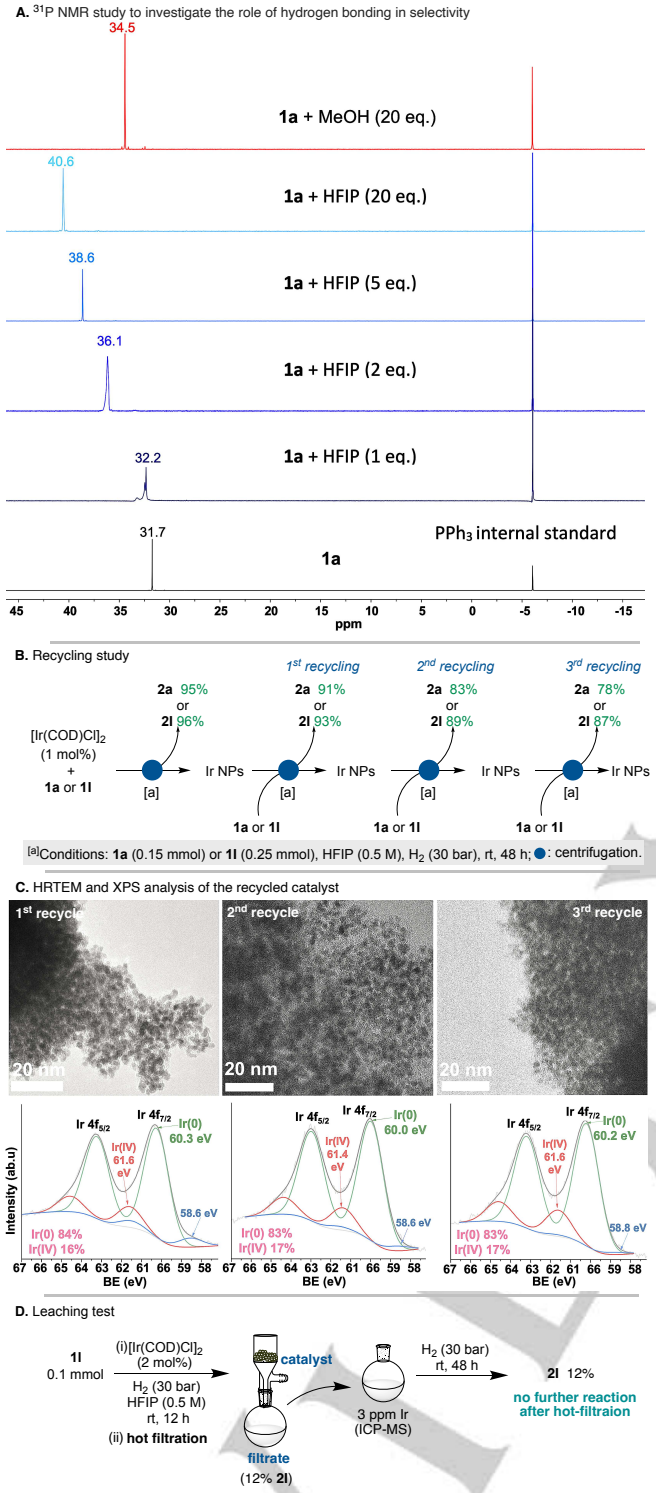

Scheme 3. (A). ^{31}P NMR study to validate hydrogen bonding between HFIP and substrate; (B). Catalyst recycling in parallel; (C) HRTEM and XPS analysis of the recycled catalyst; (D) Control hot filtration study.

Furthermore, to demonstrate the reproducibility and scalability of the methodology, we prepared an enantiopure H_8-BINAPO **2l** on a larger scale (Scheme 2A). Parallel hydrogenation of **1l** (10 times) was achieved, and ca. one gram of the desired H_8-BINAPO ligand was obtained in excellent yield. To prove an easier access to nonracemic H_8-BINAP ligand, the reduction of (*R*)-**2l** into (*R*)-H_8-BINAP **3** was accomplished in an excellent yield while retaining the enantioselectivity from the selective ring reduction to phosphine oxide reduction steps (Scheme 2B; also see Supporting Information, pages S26). The axial chirality in the substrate was retained due to the high rotational barrier around C2-C2' bond, and the transformation occurs away from the chiral axis, so even under the hydrogenation with an achiral catalyst, the enantiomeric excess was retained.[15]

To gain insights into the reaction pathway, several control experiments were conducted. First, to understand the regioselectivity of this reaction, 3-substituted quinoline **1r** was subjected to hydrogenation. The opposite regioselectivity was obtained, and the heteroaromatic ring was reduced—the product **2r** was obtained in high yield. (Scheme 2C). The altered regioselectivity may be due to the less aromaticity value for the nitrogen atom-containing ring. In all examples shown in Table 2, the regioselectivity was dictated by the substituent on the aromatic ring, impacting the aromaticity value, and creating a more hindered environment for the catalyst. The role of HFIP was also investigated. As protic solvents enabled a higher reactivity, we hypothesized that hydrogen bonding between HFIP and the oxygen atom of the phosphine oxide modifies the electronic properties of the substrate and enhances the reaction rate. As the phosphine sulfide group is less prompt to hydrogen bonding than phosphine oxides, we replaced the phosphine oxide group with sulfide. The resulting substrate **1s** was tested for selective hydrogenation. Not even traces of the expected product **2s** was detected, revealing the importance of the hydrogen bonding with HFIP (Scheme 2D). Besides hydrogen bonding, a steric effect also plays a crucial role in determining the reactivity. As proposed in the hypothesis, due to less steric hindrance, metal-arene interaction is anticipated to be more favorable with the ring containing no substituent. To verify this point, we installed 3-anisyl (**3a**) and bromo (**3b**) substituents onto the distal rings (Scheme 2E). Both the substrates were unreactive, and only staring material was recovered, indicating that the electronic and steric effects govern the reaction.

To further support the impact of hydrogen bonding on the electronic environment in the substrate, we conducted control ^{31}P NMR experiments. A significant deshielding and the downfield shift of the ^{31}P signal was observed when 20 equivalents HFIP (as an optimal amount) were added to substrate **1a** ($\Delta\delta$ = 8.9 ppm), compared to lesser deshielding upon addition of MeOH ($\Delta\delta$ = 2.8 ppm). This suggests a significant alteration of the electronic properties of the phosphine oxide substrate, which likely affects the aromaticity of the naphthalene rings and the steric environment on one ring, leading to selective reduction (Scheme 3A; also see Supporting Information, Figures S1, S2 and Table S6). Based on control NMR study, compared to methanol, HFIP forms stronger intermolecular H-bonding with the substrate and, thus, acts as a better solvent.

The catalyst recycling was also explored for two substrates (Scheme 3B, also see Supporting Information, Scheme S10). After the selective reduction of **1a**, NPs were isolated and then engaged in another hydrogenation reaction of **1a**. Surprisingly, the reactivity was only slightly affected, and the reduction of **1a** occurred with 91% conversion. The second and third recycling only afforded 83% and 78% conversions. Likewise, recycling was also achieved while synthesizing **2l** H_8-BINAP(O). Compared to the catalyst recycling using **1a**, the reduction in yield was less in each recycling when **1l** was used as substrate. This was due to

the increase in reaction scale, i.e., 0.25 mmol instead of 0.15 mmol. The slight decrease in reactivity is attributed to the slight oxidation of Ir(0) during air exposure and the slight mass loss of the catalyst during filtration. Nonetheless, this experiment supported the potential recyclability of the catalyst.

We also characterized the recycled catalyst by HRTEM, EDS, and XPS. In all recycled catalysts (Scheme 3C), NPs size remained average of ca. 2 nm, while a 1% increase in Ir(IV) amount was observed in the second recycle. The recycled catalyst still contains 83% Ir(0), as found in XPS. Also, the heterogeneous nature of the catalyst was established by the control hot filtration study (Scheme 3D, also see Supporting Information, pages S43). The substrate **1l** was exposed to catalysis for 12 h. 12% product **2l** was achieved after 12 h. The hot filtration was performed for the reaction mixture after 12 h, and the filtrate was re-subjected to a hydrogen atmosphere for the next 48 h. No further conversion of **1a** to **2a** was detected, and the mixture only contained 12% of **2l**. The same reaction mixture was also analyzed for trace Ir by ICP-MS analysis. Only ca. 3 ppm Ir was detected in the mixture, revealing the heterogeneous nature of the catalyst.

Conclusion

We described the first example of regioselective hydrogenation of (naphthyl)phosphine oxides or phosphonates using in-situ formed Ir(0) NPs in low amounts. This practical methodology offers new opportunities to quickly access enantiopure H_8-BINAPO- or H_8-BINAP-type important ligand derivatives from commercially available inexpensive BINAP ligands. The reaction starts from Ir(0), most likely generated from the in-situ reductive elimination of the hydride of Ir. The catalyst can be recycled, but with a slight decrease of reactivity, attributed to the generation of IrO_2.

Acknowledgements

For the metal-solvent aggregation study described in this paper, S.H. is grateful to the U.S. National Science Foundation for financial support (CHE-2044778). SH performed all the work at the University of Louisville.

Keywords: Hydrogenation • Iridium • Ligands • Nanoparticles • Phosphine oxides.

Conflict of interest: The authors declare no conflict of interest.

[1] a) D.-S. Wang, Q.-A. Chen, S.-M. Lu, Y.-G. Zhou, *Chem. Rev.* **2012**, *112*, 2557–2590; b) M. P. Wiesenfeldt, Z. Nairoukh, T. Dalton, F. Glorius, *Angew. Chem. Int. Ed.* **2019**, *58*, 10460–10476

[2] a) J.-H. Xie, S.-F. Zhu, Q.-L. Zhou, *Chem. Rev.* **2011**, *111*, 1713–1760; b) C. S. G. Seo, R. H. Morris, *Organometallics* **2019**, *38*, 47–65; c) R. A. A. Abdine, G. Hedouin, F. Colobert, J. Wencel-Delord, *ACS Catal.* **2021**, *11*, 215–247.

[3] Y. Wei, B. Rao, X. Cong, X. Zeng, *J. Am. Chem. Soc.* **2015**, *137*, 9250–9253.

[4] a) M. P. Wiesenfeldt, Z. Nairoukh, W. Li, F. Glorius, *Science* **2017**, *357*, 908–912; b) M. P. Wiesenfeldt, T. Knecht, C. Schlepphorst, F. Glorius, *Angew. Chem. Int. Ed.* **2018**, *57*, 8297–8300; c) M. Wollenburg, D. Moock, F. Glorius, *Angew. Chem. Int. Ed.* **2019**, *58*, 6549–6553. d) Z. Nairoukh, M. Wollenburg, C. Schlepphorst, K. Bergander, F. Glorius, *Nat. Chem.* **2019**, *11*, 264–270; e) D. Moock, T. Wagener, T. Hu, T. Gallagher, F. Glorius, *Angew. Chemie Int. Ed.* **2021**, *60*, 13677–13681.

[5] Z. Chen, C. S. Wannere, C. Corminboeuf, R. Puchta, P. von R. Schleyer, *Chem. Rev.* **2005**, *105*, 3842–3888.

[6] a) A. F. Borowski, S. Sabo-Etienne, B. Donnadieu, B. Chaudret, *Organometallics* **2003**, *22*, 1630–1637; b) S. Urban, N. Ortega, F. Glorius, *Angew. Chem. Int. Ed.* **2011**, *50*, 3803–3806; c) R. Kuwano, R. Ikeda, K. Hirasada, *Chem. Commun.* **2015**, *51*, 7558–7561; d) Y. Jin, Y. Makida, T. Uchida, R. Kuwano, *J. Org. Chem.* **2018**, *83*, 3829–3839.

[1] M. Wollenburg, A. Heusler, K. Bergander, F. Glorius, *ACS Catal.* **2020**, *10*, 11365–11370.

[7] Y. He, J. Tang, M. Luo, X. Zeng, *Org. Lett.* **2018**, *20*, 4159–4163.

[8] H. Li, Y. Wang, Z. Lai, K.-W. Huang, *ACS Catal.* **2017**, *7*, 4446–4450.

[9] D. J. Cram, R. C. Helgeson, S. C. Peacock, L. J. Kaplan, L. A. Domeier, P. Moreau, K. Koga, J. M. Mayer, Y. Chao, *J. Org. Chem.* **1978**, *43*, 1930–1946.

[10] A. Korostylev, V. I. Tararov, C. Fischer, A. Monsees, A. Börner, *J. Org. Chem.* **2004**, *69*, 3220–3221.

[11] Y. Wang, Z. Chang, Y. Hu, X. Lin, X. Dou, *Org. Lett.* **2021**, *23*, 1910–1914.

[12] a) T. Chen, C. Foo, S. C. E. Tsang, *Chem. Sci.*, 2021, **12**, 517-532; b) Y. Tarutani, M. Kudo, *J. Less-Common Met*. **1977,** *55*, 221-229; c) C. H. Suresh, N. Koga, *J. Phy. Chem. A*, **2001,** *105*, 5940-5944.

[13] J. W. Arblaster, *Platin. Met. Rev.* **2010**, *54*, 93–102.

[14] a) X. Zhang, K. Mashima, K. Koyano, N. Sayo, H. Kumobayashi, S. Akutagawa, H. Takaya, *Tetrahedron Lett.* **1991**, *32*, 7283–7286; b) X. Zhang, K. Mashima, K. Koyano, N. Sayo, H. Kumobayashi, S. Akutagawa, H. Takaya, *J. Chem. Soc. Perkin Trans.* **1994**, *1,* 2309–2322; c) M. M. Pereira, M. J. F. Calvete, R. M. B. Carrilho, A. R. Abreu, *Chem. Soc. Rev.* **2013**, *42*, 6990–7027.

15] a) M. Kranz, T. Clark, P. v. R. Schleyer, *J. Org. Chem.* **1993**, *58*, 3317–3325; b) J. Sanz García, C. Lepetit, Y. Canac, R. Chauvin, M. Boggio-Pasqua, *Chem. Asian J.* **2014**, *9*, 462–465.

Entry for the Table of Contents

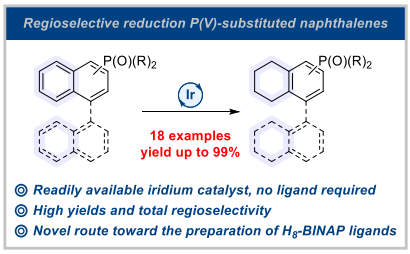

The first highly regioselective hydrogenation of P(V)-substituted naphthalenes through ligand-free iridium(0) nanoparticle catalysis is described. This novel pathway allows the formation of both new and well-established H_8-BINAP ligand-types.

Twitter Handles: @MizzouChem; @UofLChem